University of Kent

Kent Academic Repository

Beiu, Roxana M., Duma, Virgil-Florin, Mnerie, Corina A., Beiu, Andrea-Claudia, Dochia, Mihaela A., Copolovici, Lucian, Dobre, George, Bradu, Adrian and Podoleanu, Adrian (2022) *Optical coherence tomography versus microscopy for the study of Aloe Vera leaves*. In: Proceedings Volume 12138, Optics, Photonics and Digital Technologies for Imaging Applications VII. Proceedings Volume 12138, Optics, Photonics and Digital Technologies for Imaging Applications VII. . SPIE ISBN 978-1-5106-5152-4. E-ISBN 978-1-5106-5153-1.

Downloaded from

https://kar.kent.ac.uk/97310/ The University of Kent's Academic Repository KAR

The version of record is available from

https://doi.org/10.1117/12.2620766

This document version

Author's Accepted Manuscript

DOI for this version

Licence for this version

CC BY (Attribution)

Additional information

Versions of research works

Versions of Record

If this version is the version of record, it is the same as the published version available on the publisher's web site. Cite as the published version.

Author Accepted Manuscripts

If this document is identified as the Author Accepted Manuscript it is the version after peer review but before type setting, copy editing or publisher branding. Cite as Surname, Initial. (Year) 'Title of article'. To be published in ***Title of Journal*** , Volume and issue numbers [peer-reviewed accepted version]. Available at: DOI or URL (Accessed: date).

Enquiries

If you have questions about this document contact ResearchSupport@kent.ac.uk. Please include the URL of the record in KAR. If you believe that your, or a third party's rights have been compromised through this document please see our Take Down policy (available from https://www.kent.ac.uk/guides/kar-the-kent-academic-repository#policies).

Optical Coherence Tomography versus Microscopy for the Study of Aloe Vera Leaves

Roxana M. Beiu[a], Virgil-Florin Duma[a,b,*], Corina A. Mnerie[a], Andrea-Claudia Beiu[c], Mihaela A. Dochia[d], Lucian Copolovici[a,d], George Dobre[e], Adrian Bradu[e], Adrian Podoleanu[e]

[a]3OM Optomechatronics Group, *Aurel Vlaicu* University of Arad, Str. Elena Drăgoi No. 2, Arad 310330, Romania
[b]Doctoral School, Polytechnic University of Timisoara, 1 Mihai Viteazu Ave., Timisoara 300222, Romania
[c]Eindhoven University of Technology, 5600 MB Eindhoven, Netherlands
[d]Institute for Research, Development and Innovation in Technical and Natural Sciences, *Aurel Vlaicu* University of Arad, Str. Elena Drăgoi No. 2, Arad 310330, Romania
[e]Applied Optics Group, School of Physical Sciences, University of Kent, Canterbury CT2 7NH, UK

ABSTRACT

The aim of this study is to compare the advantages and limitations of two optical methods, namely Optical Coherence Tomography (OCT) and microscopy for the investigation of the structure of Aloe Vera leaves. Microscopy has the advantage of a higher resolution, but the disadvantage that the object under investigation is completely damaged (as the leaf must be removed for sample preparation). On the contrary, an advantage of OCT is that it is non-invasive with the potential added benefit of on-site measurements (if portable). The main limitation of OCT is the achievable resolution, which might not be good enough to reveal the detailed structure of noteworthy parts of leaves, for example, their stomata. The present study experimentally compares Aloe Vera data obtained using an optical microscope at different magnifications, and an in-house Swept Source (SS) OCT system with a 1310 nm center wavelength. For gathering additional information, an analysis of the normalized A-scan OCT images was also performed. This reveals additional parts of the leaf structure, while it still falls short of what can be obtained by using optical microscopy.

Keywords: Optical Coherence Tomography (OCT), microscopy, biomedical imaging, leaves cell structure, stomata, Aloe Vera, biology.

1. INTRODUCTION

Optical imaging fulfills its potential by using numerous techniques, including Atomic Force Microscopy (AFM), Scanning Electron Microscopy (SEM), Confocal Microscopy (CM), hyperspectral and reflectance microspectroscopy.

Optical Coherence Tomography (OCT) is one of these imaging techniques [1,2]. It has numerous applications in the study of different anatomical parts (including the morphology and physiology of the eye [3], skin [4], or ear [5]) and in nondestructive testing (NDT), for example for paint and faience [1]. We utilized OCT versus SEM in the profilometry of metallic surfaces, to investigate ductile, brittle, or fatigue fractures [8]. Other applications include investigations of dental materials [9,10], as well as the oral cavity [10]11-14]. In this field, we have explored OCT versus the gold standard of X-ray radiography, demonstrating that, despite its limited penetration depth (1 to 2 mm in tissue), there is a complementarity of OCT and radiography [14]. Also, higher resolution OCT (10 to 2 μm, axial) can be utilized to optimize the lower resolution (150 to 75 μm) dental radiography [14].

Based on low coherence interferometry that uses near IR laser radiation, OCT is a non-invasive method commonly capable of achieving 10 μm (and even sub-micrometer [15]) axial resolution in tissue. Besides this, OCT offers applications for

* Email: duma.virgil@osamember.org; phone: +40-751-511451; sites: http://3om-group-optomechatronics.ro/; https://www.researchgate.net/lab/3OM-Optomechatronics-Group-Virgil-Florin-Duma

in-situ measurements. Handheld scanning OCT probes have been developed in the last decade [16], for point-of-care [17], investigations of the oral cavity [14], tympanic membrane and middle ear [14]20], etc.

OCT has also applications in biological measurements of plant anatomy for distinguishing their diseases or evaluation of crops **Error! Reference source not found.**-25]. The structure of a biological sample exhibits different refractive indexes, which in turn affect the two optical path lengths of the OCT interferometer. OCT maps the structure of the sample based on its variations as depth-resolved cross-sections, known as A-scan images.

2. LEAVES IMAGING

Numerous methods have been used in biology to obtain the morphology and to study the physiology of the plant, as pointed out in Table 1. On one hand, microscopy and SEM have been useful for detailed analysis of structural features of plants, but involve vast sample preparation (e.g., sectioning, dehydration, and staining) which alters the plants **Error! Reference source not found.**. On the other hand, non-invasive techniques (e.g., nuclear magnetic resonance, X-ray, or CT) have relatively low resolution, hence are not able to reveal cell-level plant morphology. Additionally, these methods employ large and expensive devices. Likewise, there are spectroscopic methods measuring different elements of plants; however, they do not offer the possibility of depth-resolved, non-invasive imaging at the cellular level.

Leaf morphology offers a path to a better understanding of the multiple processes occurring inside plants **Error! Reference source not found.**. Optical methods have been used to determine the intimate structure of leaves, as light has long been employed for visualizing not only surfaces but also the small depths beneath them. As with any light scattering materials, the optical properties of leaves vary with their refractive indices (e.g., cell-cell and cell wall-air boundaries) **Error! Reference source not found.**26,27].

The main advantage of OCT is its non-invasiveness, which recommends this method for *in-vivo* analysis of stomata, an important part of a leaf. It is well-known that any environmental changes can have major implications on plant stress [29],29], therefore by measuring and analyzing particular changes in plant structures, one can identify environmental modifications. In this context, the interest in portable non-invasive devices for monitoring leaves becomes compelling.

Table 1. Optical methods & characteristics for analyzing leaf structure in literature.

Method	**Optical characteristics / laser source wavelength**	**Resolution**	**References**
Scanning Electron Microscopy (SEM)	Magnification:10 to 3,000,000 times	1-4 nm	**Error! Reference source not found.**,28]
Imaging (Hyper/Multi - spectral) Spectroscopy	500 – 1100 nm	~0.19 super-pixels	[30],31]
Fourier Transform Infrared Reflectance Microspectroscopy	3300 – 3600 nm	25 μm	[32]
RGB Imaging	RGB	2454 × 2056 pixels 8-bit RGB images	[33]
Thermography	7.5 – 14 μm	640 × 480 pixels	[33-35]
X-ray Dark-Field Microscopy	X-ray	Sub microns	[36]
Fluorescence, Polarimetric & Microscopy	330 nm, 470 nm, 510 nm	200 nm	[37]
STED Imaging Microscopy	pulsed STED lasers (595, 775 nm)	40 nm	[38]
Confocal Microscopy (CM)	488 nm, 561 nm	170 nm	[28],26]
Optical Coherence Tomography (OCT)	820 nm, 1050 nm, 1310 nm	3-20 μm	[1]-25] **Error! Reference source not found.**

The aim of our present, on-going study is to compare the advantages and limitations of OCT and microscopy, as well as to evaluate the A-scan, B-scan (2D/cross-section), and 3D images/volumetric reconstructions of Aloe Vera leaves investigated with OCT versus images obtained by optical microscopy (the latter, at different magnifications).

3. MATERIALS AND METHODS

3.1 Plant description

For the present investigations we choose *Aloe Vera*, a genus of a flowering succulent plant of approximately 2 years old. *Aloe Vera* morphology was investigated as early as 1908 by Berger **Error! Reference source not found.**. Later, in 1947, Matzke **Error! Reference source not found.** looked at *Aloe Vera* cells' shape arrangements. In 2014, Silva et al. studied the *Aloe Vera* leaves' morphology and water use efficiency **Error! Reference source not found.**. They determined not only the stomatal density in the abaxial and adaxial leaf regions, but also the stomata dimensions through SEM.



(a) (b)

Figure 1. (a) *Aloe Vera* plant; (b) part of the plant utilized for the present investigations.

3.2 Optical microscopy imaging

The surface morphology of *Aloe Vera* leaves was imaged by using a Zeiss Scope A1 microscope equipped with the AxioCam MRc 5 camera and controlled by ZEN lite 2012 software. For sample preparation, the upper leaf epidermis was peeled off (thickness ~20 μm), and the transparent area was spread flat in distilled water on a glass slide and pressed slightly with a coverslip. This was observed under the microscope at 50×, 100×, and 400× magnifications.

The dimensions of the inspected area at each magnification are presented in Table 2.

Table 2. Sizes of the imaged areas for different magnifications.

Magnification	Size of Measured Area
50 ×	2.8 × 2.0 (5.6 mm^2)
100 ×	1.4 × 1.0 (1.4 mm^2)
400 ×	0.4 × 0.3 (0.12 mm^2)

3.3 The OCT system

The OCT investigations were carried out using an in-house developed Swept Source (SS) OCT system (Fig. 2), enhanced by Master-Slave (MS) interferometry [42]. This OCT system has a 50 kHz laser SS (Axsun Technologies Ltd.) centered at $\lambda = 1310$ nm, with a range of $\Delta\lambda = 50$ nm. The laser output (with an optical power of 18 mW) is focused towards an 80/20 directional coupler. 20% of the beam is headed towards the bidirectional galvoscanners (GSs) [43], hence towards the sample through an optical system (NA $= 0.41$). The remaining 80% of the beam is directed towards a fixed mirror, in the reference arm. The light passing through the sample arm is reflected and refracted, while the backscattered photons re-enter into the optical system through the same path, and interfere with those from the reference arm. The resulting light is sensed by a balanced photodetector (Santec Model BPD-200 DC), and converted into electrical signals, which are digitized by a 12 bit, 500 MS/s waveform digitizer model, ATS9350 (Alazartech). These signals are visualized using a LabView-based software package, in-house developed [42], which also controls the 2D GS through a data acquisition

board, model PCI 6110 (National Instruments). The wavelength spectra acquired are recorded as A-scans, respectively, from which B-scans images are obtained by using the Master-Slave protocol. The system control and the signal acquisition are achieved using the LabView software, and the saved images are post-processed to construct a 3D OCT image, as well as *en-face* images located at a wavelength-specific depth into the sample - Fig. 4(d,e,f). The measurements on the *Aloe Vera* leaves were completed for three different amplitudes of the GS (denoted by A_1, A_2, A_3), which correspond to three scanned areas of the sample: 0.75×0.75 mm^2, 1.5×1.5 mm^2, and 2.25×2.25 mm^2, respectively (Table 3). The OCT system has axial (Δx) and lateral (Δz) resolutions (in air), as follows [44]:

$$\Delta x = 0.37 \cdot \frac{\lambda_0}{NA} = 1.2\ \mu\text{m} \quad (1)$$

$$\Delta z = \frac{2 \cdot \ln 2}{\pi} \cdot \frac{{\lambda_0}^2}{\Delta\lambda} = 10.6\ \mu\text{m}. \quad (2)$$

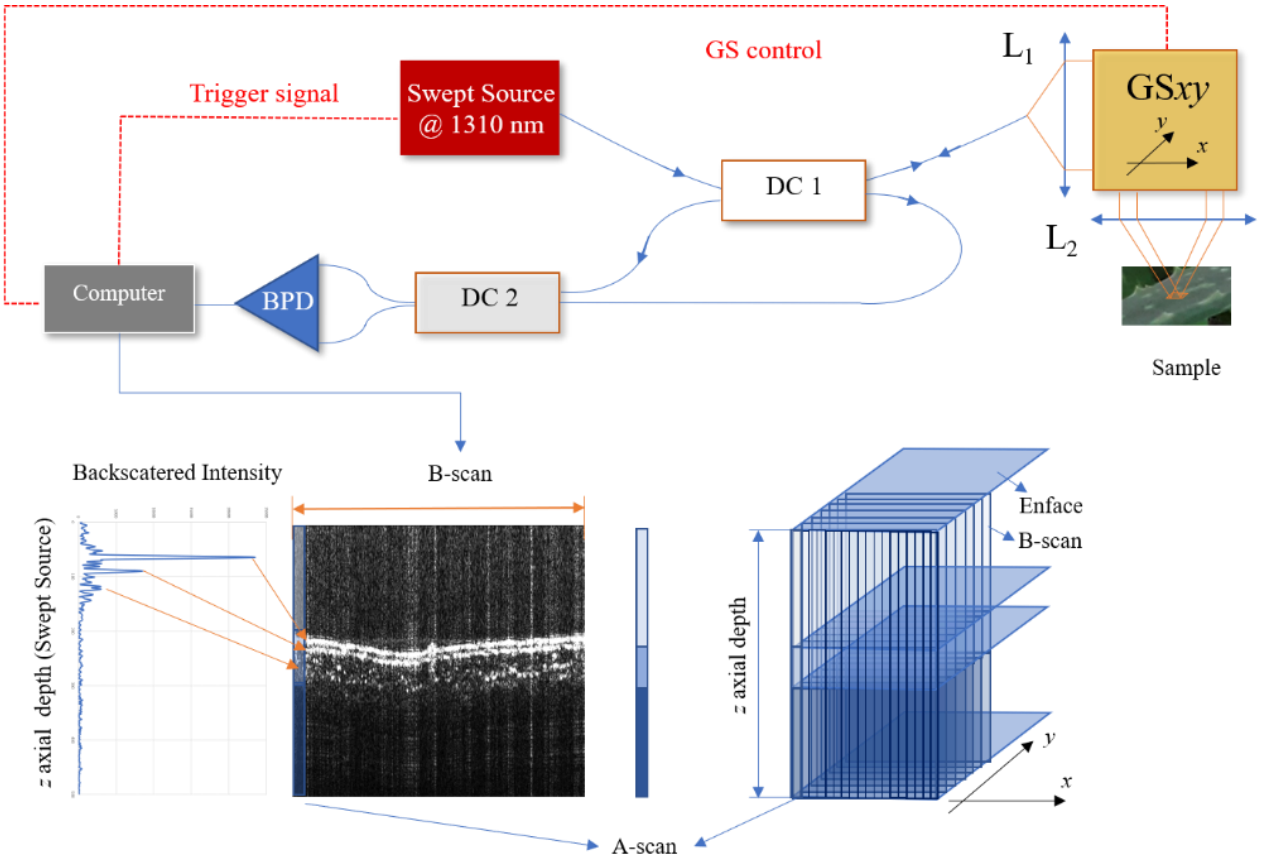


Figure 2. Schematics of the OCT system, acquisition and processing of images: $DC_{1,2}$ single mode directional couplers (20/80 and 50/50, respectively); GS_{xy}, dual axis 2D galvanometer scanner; $L_{1,2}$, achromatic lenses; BPD, balanced photodetector.

Depending on the amplitude ($A_i, i = 1, 2, 3$) of the GS, the area under measurements varies accordingly. Table 3 shows image sizes in accordance with the respective A_i value. The images comparison was done on the adjusted area, by cropping the original size of the OCT cross section to be as close as possible to that of the microscopy image.

Table 3. Sizes of the areas imaged using the OCT system.

Amplitude (A_i)	**Size of Measured Area**	**Cropped Area (A_{2crop})**
A_1	0.75×0.75 (0.562 mm^2)	
A_2	1.5×1.5 (2.250 mm^2)	1.5×1.0 (1.5 mm^2)

A_3	2.25 × 2.25 (5.062 mm^2)	

4. IMAGE COMPARISON

The process of comparing images required several steps. The first one was to choose the right size of the images. We choose the image of 100 × magnification (1.4 × 1.0 mm^2) to be compared with the adjusted (cropped) cross-section OCT image, $A_{2\text{crop}} = (1.5 \times 1.0\ \text{mm}^2)$, from Tables 2 and 3, respectively. The second step included processing the cross-section of optical microscopy images by using ZEN lite 2012, as well as OCT images by using ImageJ.

We used one of the ImageJ processing features, namely pseudocolor image Look-Up Tables (Fig. 3). In such a way, images with differences in color in the pseudo-colored acquired images (from OCT system acquisition board) will "reflect differences in intensity of the object rather than differences in the color of the specimen that has been imaged") [45].

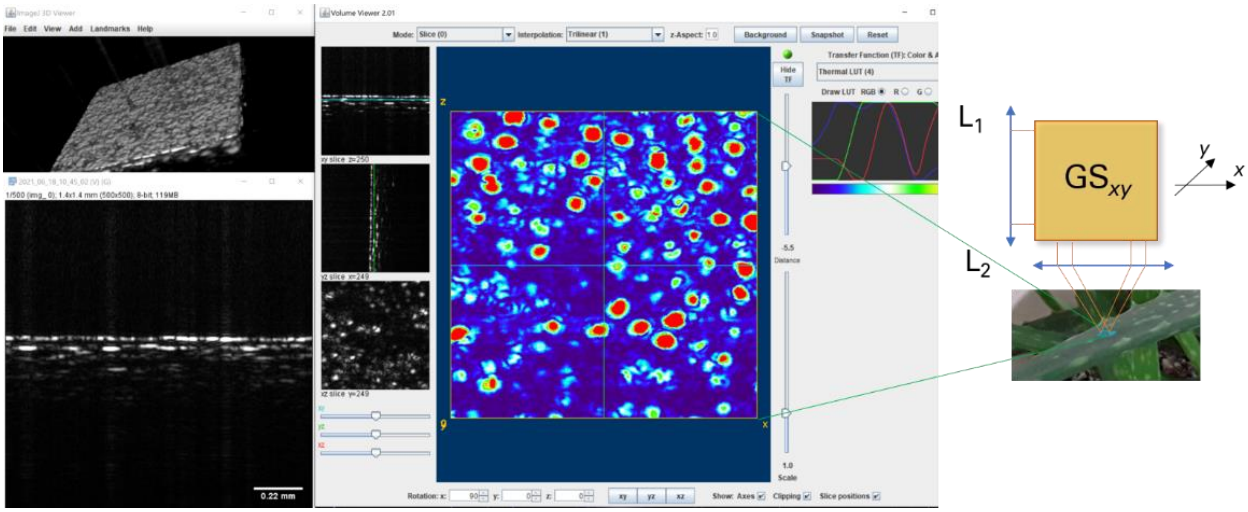
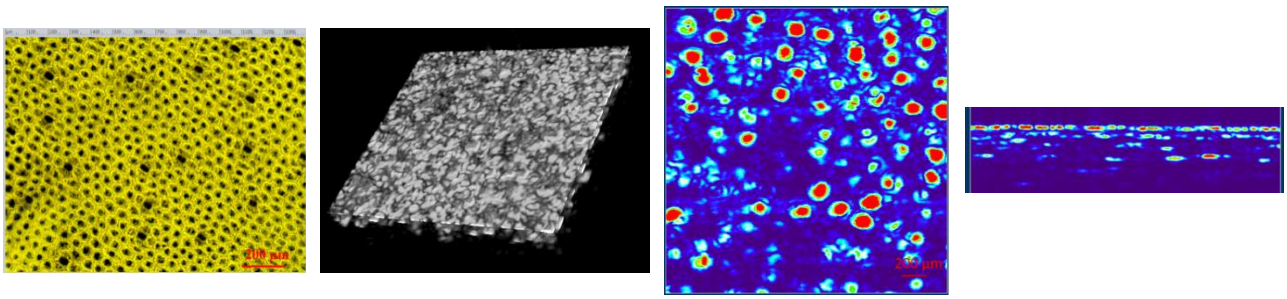


Figure 3. Right side: a sketch of the GS_{xy} (where $L_{1,\,2}$, are lenses) and the *Aloe Vera* plant scanned area; Left side has ImageJ windows: left down is one of the 500 B-scans, left up is a 3D image Viewer, and in the center is the Volume Viewer window (the LUT pseudo-color of a cross section area at a depth of ~ 20 μm, see green lines).

The stomata which can be seen in Fig. 4a are visible with large, black dotted shapes. These shapes are similarly detected in the processed cross-section 3D-OCT images as large, red circular areas (Fig. 4c). There is not a perfect match between these two images because we imaged different parts of *Aloe Vera* leaf with optical microscopy and OCT respectively. A perfect match is hard to obtain as this would require not only using the same portion of the same leaf but also aligning it in the same way in those two different optical systems.

The third step is to make a correlation between the set of microscopy image (magnification 100 ×) and the processed cross-section OCT images/B-scan (for A_2 and a depth of ~20 μm).



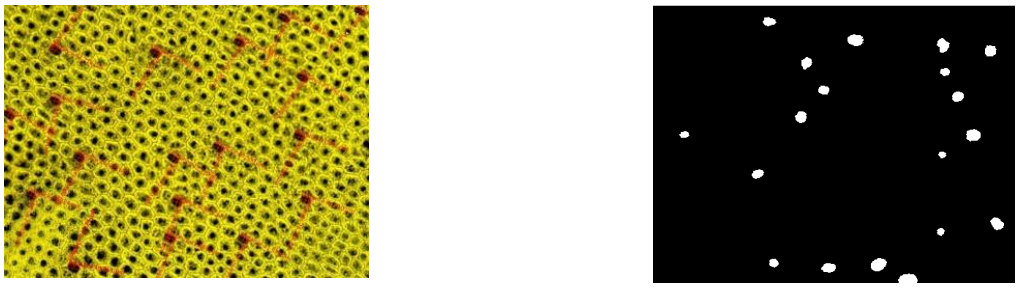
(a) (b) (c) (d)

Figure 4. Optical microscopy images: (a) 100 × magnification, area of 1.4 × 1.4 mm^2, (b) 3D-OCT image for A_2 scanned area; (c) ImageJ LUT post-processed cross-section (xy plane); (d) same as (c) for the (yz) plane.

5. RESULTS

The optical microscopy image (100 ×) was analyzed using ZEN lite 2012, and we determined the dimensions and number of stomata on the specific sample (Fig. 5a). The analyzed OCT image (Fig. 4h) was processed through color thresholds and segmentation using Matlab Image Processing (Fig. 5b). In this way, we determined the values of major and minor axes of segmented areas for both images.

For the optical microscopy image (Fig. 5a) there are 18 number of oval-like shapes. In Matlab Image Processing Toolbox (Color Depth and Segmentation), we filtered the OCT cross section image to achieve the same number of stomata, based on the studied area (Fig. 5b). The major and minor axis length and area of these shapes were automatically computed (Table 4).



(a) (b)

Figure 5. (a) Microscopy image from Fig. 4a; (b) Color threshold processed image from Fig. 4c.

Table 4. Computed values of oval-like shape: major axis, minor axis and area

Microscopy data				Matlab Image processing of cross-section OCT Data		
# Shapes	Major axis length (pixels)	Minor axis length (pixels)	Area (oval-like shape): A_M	Major axis length (pixels)	Minor axis length (pixels)	Area (oval-like shape): A_{OCT}
1	14.663	8.702	100.218	10.771	10.068	83
2	15.471	8.520	103.519	13.253	9.126	93
3	14.850	9.561	111.514	13.626	10.743	113
4	15.254	9.541	114.299	13.166	11.678	119
5	15.407	9.541	115.450	15.513	12.306	148
6	13.866	10.704	116.563	17.079	11.629	154
7	15.496	9.724	118.350	18.028	11.807	162
8	16.808	9.249	122.089	16.795	13.666	176
9	15.697	10.197	125.711	16.744	13.800	180
10	15.697	10.274	126.658	16.451	15.164	193
11	14.892	10.939	127.949	16.314	15.372	194
12	14.889	10.957	128.130	19.981	12.791	198
13	15.970	10.274	128.859	19.609	14.762	223
14	16.250	10.120	129.154	19.763	15.551	230
15	14.311	11.516	129.443	20.466	16.400	260
16	15.970	10.777	135.171	22.097	15.722	270
17	16.808	11.819	156.015	22.623	16.649	294
18	17.518	12.260	168.687	27.638	14.466	304

6. DISCUSSION AND CONCLUSIONS

By comparing the cross-section OCT images of Aloe Vera with optical microscopy images we were able to determine in this on-going study the stomata structure (i.e., shape and number). It could be concluded from this preliminary study that, by choosing the same area for comparison, the size of stomata looks to be almost the same. The main advantage of leaf structure analysis by OCT is the non-invasiveness. Also, an important aspect is that *in-vivo* measurements are possible; so are on-site measurements, with for portable OCT systems [20,21], equipped with handheld scanning probes [20].

The leaf structure is the center of the physiological function. It is responsible for the different responses in metabolical, physiological, and ecological responses of plants to various conditions, including biotic and abiotic stresses. The determination of leaf anatomical traits (such as stomata size, density, or distribution) could provide important morphological and cytological information regarding the stage of the leaf and/or its physiological functionality **Error! Reference source not found.**.

In this study we compared two optical methods, OCT and optical microscopy, when analyzing the structure of Aloe Vera leaves. On one side, microscopy has the advantage of a higher resolution, but the main disadvantage is that the object under investigation is completely damaged. On the other side, the main advantage of OCT is that it is non-invasive and has the possibility of on-site measurements (if portable). The main disadvantage of OCT (potentially more so for portable systems) is the achievable resolution, which might not be good enough to reveal the detailed structure of parts of leaves, for example, their stomata. This is why the present study compared *Aloe Vera* images obtained using an optical microscope at different magnifications, and an in-house developed MS/SS-OCT system with a 1310 nm center wavelength. By analyzing the images recorded with these two optical methods, we obtained so far a good visual match between OCT and microscopy regarding stomata shape and number.

To have a confirmation of these incipient results we must measure a higher number of samples. Also, our future work continues not only on *Aloe Vera* leaf measurements but also expanding the plant types, as it is well known that leaf morphology is specific to each plant.

ACKNOWLEDGEMENTS

This research was supported by the Romanian Ministry of Research, Innovation and Digitization, CNCS/CCCDI–UEFISCDI, project PN-III-P4-ID-PCE-2020-2600, within PNCDI III. A.B. and A.P. acknowledge the support of the European Research Council (http://erc.europa.eu), Grant 249889 and of the Biotechnology and Biological Sciences Research Council (BBSRC) grant BB/S0166431/1 and Engineering and Physical Sciences Research Council (EPSRC) grant Rebot EP/N019229/1. A.P. is also supported by the NIHR Biomedical Research Centre at Moorfields Eye Hospital NHS Foundation Trust and UCL Institute of Ophthalmology, and by the Royal Society Wolfson Research Merit Award.

AP and AB acknowledge the support of Biological Sciences Research Council (BBSRC), “5DHiResE” project, BB/S016643/1; AP also acknowledges the European Union’s Horizon 2020 research and innovation programme under the Marie Sklodowska-Curie grant NETLAS (agreement No 860807). AP further acknowledges the National Institute for Health Research Biomedical Research Centre at Moorfields Eye Hospital NHS Foundation Trust (NIHR), the UCL Institute of Ophthalmology, University College London (AP) and the Royal Society Wolfson research merit award.

REFERENCES

[1] Huang, D., Swanson, E. A., Lin, C. P., Schuman, J. S., Stinson, W. G., Chang, W., Hee, M. R., Flotte, T., Gregory, K., Puliafito, C. A. and Fujimoto, J. G., "Optical coherence tomography, " Science 254(5035), 1178-1181 (1991).

[2] Adler, D.C., Chen, Y., Huber, R., Schmitt, J., Connolly, J., Fujimoto, J.G., "Three-dimensional endomicroscopy using optical coherence tomography, " Nature Photonics 2007; 1: 709–16.

[3] Mehreen, A., Duker, J.S., "Optical coherence tomography–current and future applications, " Curr. Opin. Ophthalmol. 2013, 24, 213–221.

[4] Gambichler, T., Jaedicke, V., Terras, S., "Optical coherence tomography in dermatology: Technical and clinical aspects, " Arch. Derm. Res. 2011, 303, 457–473.

[5] Cogliati, A., Canavesi, C., Hayes, A., Tankam, P., Duma, V.-F., Santhanam, A., Thompson, K.P., Rolland, J.P., "MEMS-based handheld scanning probe for distortion-free images in Gabor-Domain Optical Coherence Microscopy, " Opt. Express 2016, 24, 13365–13374.
[6] Read, M., Cheung, C.S., Liang, H., et al., "A Non-invasive Investigation of Egyptian Faience Using Long Wavelength Optical Coherence Tomography (OCT) at 2 μm," Studies in Conservation, (2021).
[7] Hutiu, G., Duma, V.-F., Demian, D., Bradu, A., Podoleanu, A.G., "Surface imaging of metallic material fractures using optical coherence tomography, " Applied Optics 53(26), 5912-5916 (2014).
[8] Hutiu, G., Duma, V.-F., Demian, D., Bradu, A., Podoleanu, A.G., "Assessment of Ductile, Brittle, and Fatigue Fractures of Metals Using Optical Coherence Tomography," Metals 8(2), 117 (2018).
[9] Isfeld, D.M., Aparicio, C., Jones, R.S., "Assessing near infrared optical properties of ceramic orthodontic brackets using cross-polarization optical coherence tomography," J. Biomed. Mater. Res. B Appl. Biomater. 102, 516–523 (2014).
[10] Duma, V.-F., Sinescu, C., Bradu, A., Podoleanu, A., "Optical Coherence Tomography Investigations and Modeling of the Sintering of Ceramic Crowns," Materials 12(6), 947 (2019).
[11] Otis, L., Everett, M. J., Sathyam, U.S., Colston Jr., B. W., "Optical Coherence Tomography: A New Imaging: Technology for Dentistry," The J. of the American Dental Association 131(4), 511-514 (2000).
[12] Hsieh, Y.-S., Ho, Y.-C., Lee, S.-Y., Chuang, C.-C., Tsai, J., Lin, K.-F., and Sun, C.-W., "Dental Optical Coherence Tomography," Sensors 13, 8928-8949 (2013).
[13] Erdelyi, R.A., Duma, V.-F., Sinescu, C., Dobre, G.M., Bradu, A., Podoleanu, A., "Dental Diagnosis and Treatment Assessments: Between X-rays Radiography and Optical Coherence Tomography," Materials 13(21), 4825 (2020).
[14] Erdelyi, R.-A., Duma, V.-F., Sinescu, C., Dobre, G.M., Bradu, A., Podoleanu, A., "Optimization of X-ray Investigations in Dentistry Using Optical Coherence Tomography," Sensors 21(13), 4554, (2021).
[15] Drexler, W., Liu, M., Kumar, A., Kamali, T., Unterhuber, A., Leitgeb, R.A., "Optical coherence tomography today: Speed, contrast, and multimodality," J. Biomed. Opt. 19, 071412 (2014).
[16] Lu, C.D., Kraus, M.F., Potsaid, B., Liu, J.J., Choi, W., Jayaraman, V., Cable, A.E., Hornegger, J., Duke, J.S., Fujimoto, J.G., "Handheld ultrahigh speed swept source optical coherence tomography instrument using a MEMS scanning mirror," Biomed. Opt. Express 2014, 5, 293–311.
[17] Monroy, G.L., Won, J., Spillman, D.R., Dsouza, R., Boppart, St.A.," Clinical translation of handheld optical coherence tomography: Practical considerations and recent advancements," J. Biomed. Opt. 2017, 22, 121715.
[18] Demian, D., Duma, V.-F., Sinescu, C., Negrutiu, M.L., Cernat, R., Topala, F.I., Hutiu, Gh., Bradu, A., Podoleanu, A.Gh., "Design and testing of prototype handheld scanning probes for optical coherence tomography," J. Eng. Med. 228, 743–753 (2014).
[19] Duma, V.-F., Dobre, G., Demian, D., Cernat, R., Sinescu, C., Topala, F.I., Negrutiu, M.L., Hutiu, Gh., Bradu, A., Podoleanu, A. Gh., "Handheld scanning probes for optical coherence tomography," Rom. Rep. Phys. 2015, 67, 1346–1358.
[20] Won, J, Monroy, G.L., Dsouza, R.I., et al., "Handheld briefcase optical coherence tomography with real-time machine learning classifier for middle ear infections," Biosensors 11(5), 143 (2021).
[21] Wijesinghe, R.E., Lee, S.-Y., Ravichandran, N.K., et al., "Optical coherence tomography-integrated, wearable (backpack-type), compact diagnostic imaging modality for in situ leaf quality assessment," Appl. Opt. 56(9), D108-D114 (2017).
[22] Anna, T., Chakraborty, S., Cheng, C.-Y., et al., "Elucidation of microstructural changes in leaves during senescence using spectral domain optical coherence tomography," Sci. Rep. 9, 1167 (2019).
[23] Rateria, A., Mohan, M., Mukhopadhyay, K., Poddar, R., "Investigation of Puccinia triticina contagion on wheat leaves using swept source optical coherence tomography," Optik 178, 932-937 (2019).
[24] De Wit, J., Tonn, S., Van den Ackerveken, G., et al., "Quantification of plant morphology and leaf thickness with optical coherence tomography," Appl. Opt. 59(33), 10304-10311 (2020).
[25] Srimal, L.K.T., Rajagopalan, U.M., Kadono H., "Functional optical coherence tomography (fOCT) biospeckle imaging to investigate response of plant leaves to ultra-short term exposure of ozone," J. Phys.: Conf. Series 605(1), 012013 (2015).
[26] Grace, O.M., Simmonds, M.S.J., Smith, G.F., Van Wyk, A.E., "Taxonomic significance of leaf surface morphology in Aloe section Pictae (Xanthorrhoeaceae)," Botanical J. Linnean Soc. 160(4), 418-428 (2009).
[27] Silva, H., Sagardia, S., Ortiz, M., et al., "Relationships between leaf anatomy, morphology, and water use efficiency in Aloe vera (L) Burm f. as a function of water availability," Rev. Chil. Hist. Nat. 87, art. 13 (2014).

[28] Li, L., Luo, Y., Peijnenburg, W.J.G.M., Li, R., Yang, J., Zhou, Q., "Confocal measurement of microplastics uptake by plants," MethodsX 7, 100750 (2020).
[29] Urban, M.A., Barclay, R.S., Sivaguru, M., Punyasena, S.W., "Cuticle and subsurface ornamentation of intact plant leaf epidermis under confocal and superresolution microscopy," Microsc. Res. Tech. 81(2),129-140 (2018).
[30] Mishra, P., Lohumi, S., Khan, H.A., Nordon, A., "Close-range hyperspectral imaging of whole plants for digital phenotyping: Recent applications and illumination correction approaches," Comp. & Electr. Agriculture 178, 105780 (2020).
[31] Monakhova, M., Yanny, K., Aggarwal, N., Waller, L., "Spectral DiffuserCam: lensless snapshot hyperspectral imaging with a spectral filter array," Optica 7, 1298-1307 (2020).
[32] Khambatta, K., et al., "“Wax On, Wax Off”: In vivo imaging of plant physiology and disease with Fourier transform infrared reflectance microspectroscopy," Adv. Sci. 2, 01902 (2021).
[33] Elsayed, S., et al., "Combining thermal and RGB imaging indices with multivariate and data-driven modeling to estimate the growth, water status, and yield of potato under different drip irrigation regimes," Remote Sensing 13, 1679 (2021).
[34] Vialet-Chabrand, S., Lawson, T., "Thermography methods to assess stomatal behaviour in a dynamic environment," J. of Experimental Botany 71(7), 2329–2338 (2020).
[35] Zubler, A.V., Yoon, J.-Y., "Proximal methods for plant stress detection using optical sensors and machine learning," Biosensors 10(12), 193 (2020).
[36] Jensen, T.A., Bech, M., Bunk, O., et al., "Directional x-ray dark-field imaging," Phys. Med. Biol. 55 (12), 3317-3323 (2010).
[37] Van Eeckhout, A., Garcia-Caurel, E., Garnatje, T., et al., "Polarimetric imaging microscopy for advanced inspection of vegetal tissues," Sci. Rep. 11, 3913 (2021).
[38] Vicidomini, G., Bianchini, P., Diaspro, A., "STED super-resolved microscopy," Nat. Methods 15, 173–182 (2018).
[39] Berger, A., [Liliaceae-Asphodeloideae-Aloineae], in: Engler, A., Das Pflanzenreich, Im Auftrage der Konigl Preuss Akademie der Wissenschaften, Leipzig, 1-347 (1908).
[40] Matzke, E.B., "The three-dimensional shape of epidermal cells of Aloe Aristata," Amer. J. Botany 34(4), 182-195 (1947).
[41] Silva, H., Sagardia, S., Ortiz, M., et al., "Relationships between leaf anatomy, morphology, and water use efficiency in Aloe vera (L) Burm f. as a function of water availability," Rev. Chil. Hist. Nat. 87, art. 13 (2014).
[42] Podoleanu, A., Bradu, A. "Master-slave interferometry for parallel spectral domain interferometry sensing and versatile 3D optical coherence tomography," Opt. Expr. 21, 19324-19338 (2013).
[43] Duma, V.-F., "Laser scanners with oscillatory elements: Design and optimization of 1D and 2D scanning functions," Applied Mathematical Modelling 67(3), 456-476 (2019).
[44] Izatt, J.A., Choma, M.A., "Theory of optical coherence tomography," in: Drexler, W., Fujimoto, J.G. (Eds.), "Optical Coherence Tomography. Biological and Medical Physics, Biomedical Engineering," Springer, Berlin, Heidelberg (2008).
[45] https://imagej.net/imaging/visualization (accessed 28 Feb. 2022).
[46] Casson, S., Gray, J.E., "Influence of environmental factors on stomatal development," New Phytologist 178(1), 9-23 (2008).